First of all, we appreciate the reviewer's comment and suggestion. In response to them, we have made relevant revisions to the manuscript. Listed below are our answers and the changes made to the manuscript according to the question and suggestion given by the reviewer. The comment of the reviewer (in black) is listed and followed by our responses (in blue).

Effect of CCN concentration on convective precipitation formation in two case studies is presented. State of the art cloud resolving model with detailed representation for cloud microphysics is employed. The analysis highlights the role of aerosol in affecting the formation of heavy precipitation on both studied locations. In the Beijing case the analysis related to changes in surface precipitation is interesting. Especially how precipitation pattern changes towards stronger precipitation. I guess the computational cost of the simulations is relatively high, and thus ensembles with more variability in the aerosol properties cannot be employed to make the analysis stronger. Based on one pair of simulations, the uncertainty related to the overall strength of processes is high as small change in initial conditions could affect the relative aerosol effect a lot. However, how different processes and feedbacks work needs to be analyzed in more detail before I can recommend the manuscript to be accepted to be published in ACP.

It seems like the changes in condensation rate are now presented as the only reason for the increased updrafts. It goes also in opposite as stronger updrafts automatically increases also condensation rate. Increase in the aerosol concentration followed by increase in droplet concentration should not produce very significant change in the condensation rate as droplet concentration are expected to be relatively high even in the low aerosol simulations. Presenting the droplet number concentration would be thus highly beneficial. I would expect it is more likely that delayed formation of precipitation in warm processes is affecting more on liquid water content than the increased condensation through enhanced cloud droplet formation. This could also affect cloud radiative properties. Also, there is no discussion on how much column averaged condensation rates are affected by the change in the fraction of cloudy grid boxes or how for example the cloud top height is changing due to aerosol changes and cloud invigoration. The increase in condensation rate can be directly connected to increase in the precipitation like is done in the manuscript, but connecting the change in condensation rate to increased droplet number concentration requires more evidence. For example, what would happen if you just increase the condensation coefficient in low aerosol case?

We believe that this general comment is closely linked to the following specific comments below:

1. A comment on line 402
2. A comment on line 403
3. A comment on Figure 8

So, we suggest that the reviewer should look at our responses to these three comments as a way of finding our response to this general comment.

In the abstract the statement “In both of the areas, aerosol-induced changes in freezing play a negligible role in aerosol-precipitation interactions as compared to the role played by aerosol-induced changes in condensation and deposition.” is quite strong as the number of ice particles is not affected by aerosol. Thus, through the manuscript, I suggest changing the wording to be about the change in CCN instead the change in aerosol.

We changed wording following the suggestion here

The analysis of gust fronts is somewhat separated from the rest of the analysis. What is the role of droplet evaporation through the simulations in driving the instability? Especial when compared against the enhanced condensation from increased droplet concentration?

Aerosol-induced enhancement of the frequency of precipitation with rates above 12 mm hr^{-1} starts to emerge at 17:00 LST as described in Section a for the Beijing case via mechanisms associated with exchanges of the moist static energy between areas A and B as described in Section e “moist static energy”. Not only the initial small differences in the frequency of precipitation with rates above 12 mm hr^{-1} between the control-b and low-aerosol-b runs at 17:00 LST enhance substantially but also the maximum precipitation rate and its differences between the runs enhance substantially particularly during the period between 17:00 and 19:00 LST as seen in Figures 11b, 11c and 11d. Note that the establishment of the differences in the precipitation (cumulative) frequency and the maximum precipitation at 19:00 LST between the runs, followed by this substantial enhancement during the period between 17:00 and 19:00 LST, is basically equivalent to the establishment of those differences at the last time step of the runs as described in Section a for the Beijing case. Hence, we are interested in mechanisms controlling this substantial enhancement during the period between 17:00 and 19:00 LST and this is why we analyzed gust fronts and associated processes such as evaporation during the period between 17:00 and 19:00 LST as shown in Section d “evaporation and gust fronts” and why we do not take interest in the role of evaporation before 17:00 LST and after 19:00 LST.

Aerosol-induced increases in droplet evaporation make positive feedbacks with aerosol-induced increases in condensation. As described in Section b for the Beijing case, at the initial stage of cloud development before 17:00 LST, due to aerosol-induced increases in the nucleation of droplets and associated increases in the integrated surface of droplets, there are aerosol-induced increases in condensation. Then, as shown in Section d "evaporation and gust fronts", these aerosol-induced increases in condensation in turn enhance the amount of cloud liquid as a source of evaporation and then the droplet evaporation. The enhanced droplet evaporation in turn intensifies the gust fronts more, and this more intensified gust fronts in turn intensify updrafts and enhance condensation more in the control-b run than in the low-aerosol-b run during the period between 17:00 and 19:00 LST. In particular, the more enhanced condensation due to the more intensified gust fronts during the period between 17:00 and 19:00 LST in the control-b run contributes to the substantially increasing differences in the frequency of precipitation with rates above ~ 12 mm hr^{-1} between the runs, the substantially increasing maximum precipitation and its differences between the runs during the period between 17:00 and 19:00 LST.

To describe overall roles of droplet evaporation through the simulations or the whole simulation period, let me come up with the classic theory of evaporation and associated instability as follows. The following is basically about well-known classic theory, hence, we don't discuss it in text:

As well known and well described in Houze (1993) and Weisman and Klemp (1982), in the presence of wind shear, the evaporation of condensed liquid or droplets detrained to unsaturated areas and associated evaporative cooling do not align with condensation and associated condensational heating in the vertical direction. When condensational heating and evaporative cooling are vertically aligned at a similar horizontal location, the cooling stabilizes air and weakens convection. However, in the presence of wind shear as in the Beijing case, areas with evaporative cooling do not align with those with condensation heating in the vertical direction, and instead, those areas with evaporative cooling are located in different places in the horizonal domain as compared to those with condensational heating. This enables those areas with evaporative cooling can form gust fronts. These gust fronts lift surrounding warm air and generate subsequent convection via the forced-convection mechanism, and this in turn generate subsequent updrafts, condensation and precipitation. More condensation and cloud liquid as a source of evaporation induce more evaporative cooling and more intensified gust fronts in the control-b run than in the low-aerosol-b run. This formation of gust fronts and their CCN-induced intensification exist throughout the simulation period. However, roles of this formation and intensification of gust fronts in precipitation with rates above 12 mm hr^{-1} and the maximum precipitation are not significant before 17:00 LST when the MCS is at its initial stage and

after 19:00 LST when the MCS enters its decaying stage, and become significant to induce above-described substantial enhancement of differences in the frequency of precipitation with rates above 12 mm hr^{-1} and the maximum precipitation rate between the runs during the time period between 17:00 and 19:00 when the MCS is at its mature stage. During the mature stage, wind shear is stronger, hence, areas with evaporative cooling are located in different places in the horizonal domain as compared to those with condensational heating in a more effective way than during the initial and decaying stages. Therefore, during the mature stage, the formation of gust fronts is more efficient or gust fronts are formed more fully, and this enables CCN-induced more evaporative cooling to affect gust fronts more effectively. Hence, roles of the formation and intensification of gust fronts in precipitation are more substantial during the mature stage than during the initial and decaying stages.

To make a better connection between Section d about gust fronts and the other sections, a part of text in Section d is revised as follows:

(LL765-776 on p26)

As described above, the more droplet nucleation and greater integrated droplet surface induce more condensation before 17:00 LST in the control-b run. This and lower efficiency of collision and collection among droplets enable the control-b run to have a larger amount of cloud liquid or droplets as a source of evaporation. This in turn enables more droplet evaporation, more associated cooling and stronger downdrafts, although less rain evaporation is in the control-b run particularly for the period from 17:00 LST to 19:00 LST (Figure 17). More evaporation of droplets and associated stronger downdrafts with higher concentrations of aerosols acting as CCN have been shown by the numerous previous studies (e.g., Tao et al., 2007; Tao et al., 2012; Khain et al., 2008; Lee et al., 2018).

During the period between 17:00 and 19:00 LST, with the development of convergence or the gust front, as mentioned above, the maximum precipitation rate increases from ~ 17 (17) to ~ 45 (33) mm hr^{-1} in the control-b (low-aerosol-b) run (Figure 11).

(LL780-787 on p26)

Over the period from 17:00 LST to 19:00 LST, stronger downdrafts and associated stronger outflow generate a stronger gust front and more subsequent condensation in the control-b run. This enhances the small initial difference, which is at 17:00 LST, in the frequency of precipitation with rates above ~12 mm hr-1 between the runs substantially as time progresses from 17:00 LST to 19:00 LST (Figure 11). Associated with this, with the time progress, the nearly identical maximum precipitation rate

between the runs at 17:00 LST turns into the significantly higher maximum precipitation rate in the control-b run than in the low-aerosol-b run (Figure 11).

Specific comments:

Line 59: “With increasing aerosol loading or concentrations, cloud-particle sizes and autoconversion, which represent cloud microphysical properties, can be changed.” Autoconversion is not a microphysical property but a parameterized process representation to create precipitation from cloud droplets. As you have binned microphysics employed, I would expect there is no need for the autoconversion.

The word “autoconversion” is removed in text and text is revised accordingly. However, just want to mention that in the microphysical scheme adopted in this study, for the calculation of cloud liquid content and rain water content which are variables in the WRF model, drops whose radius is smaller (greater) than 40 micrometer are treated to be droplets (raindrops), although there are no separate size distributions between droplets and raindrops. Stated differently, there is only one size distribution for drops and in this size distribution, drops whose radius is smaller (greater) than 40 micrometer are treated to be droplets (raindrops) for the calculation of the WRF variables that are used in other schemes such as radiation and PBL schemes. With this treatment, autoconversion is defined to be a process where droplets, which are drops with radius smaller than 40 micrometers, collide and collect each other to form raindrops, which are drops with radius greater than 40 micrometers. This definition of autoconversion is that of autoconversion in authors’ responses below, although the word “autoconversion” is not in the manuscript anymore.

Line 192: “based on the fact that aerosol composition does not vary significantly over the domain and during the whole period with the observed clouds.” How do you know this? AERONET does not provide data in cloudy conditions.

We re-checked the AERONET data used and found that we tried to collect the AERONET data from a time point 1 hour before the observed clouds form to the end of the simulation period. However, due to the reason stated by the reviewer here, we found that the AERONET data from a time point when the clouds form to the end of the simulation period were not taken into account for calculating aerosol composition and size distribution and only those data, which are at a time point 1 hour before the observed clouds form, are considered to obtain aerosol composition and size distribution.

Accordingly, we corrected text as follows:

(LL237-241 on p9)

The AERONET data are averaged over the AERONET sites at 02:00 LST December 24th 2017 (13:00 LST July 27th 2015), which is 1 hour before the observed MCS forms, for the Seoul (Beijing) case. Based on the average data, it is assumed that aerosol particles are internally mixed with 70 (80) % ammonium sulfate and 30 (20) % organic compound for the Seoul (Beijing) case.

(LL261-264 on p9)

The distribution parameters of the assumed shape of the size distribution of background aerosols in Figure 3a (3b) are those that are averaged over the AERONET sites at a time point, which is 1 hour before the observed MCS form, for the Seoul (Beijing) case.

Line 202: Aitken mode, not nucleation

Corrected.

Line 223: IN concentration seems high, what is the temperature dependence for heterogeneous nucleation and what is the actual ice number concentration in the simulations?

To describe how nucleation processes are represented, the following is added:

(LL190-197 on p7)

A cloud-droplet nucleation parameterization based on Köhler theory represents cloud-droplet nucleation. Arbitrary aerosol mixing states and aerosol size distributions can be fed to this parameterization. To represent heterogeneous ice-crystal nucleation, parameterizations by Lohmann and Diehl (2006) and Möhler et al. (2006) are used. In these parameterizations, contact, immersion, condensation-freezing, and deposition nucleation paths are all considered by taking into account the size distribution of INPs, temperature and supersaturation. Homogeneous droplet freezing is considered following the theory developed by Koop et al. (2000).

As described in the added text, the heterogeneous nucleation is represented by parameterizations by Lohmann and Diehl (2006) and Möhler et al. (2006). The details of these parameterizations are as follows and these details are not presented in text for the sake of brevity of text:

In Lohmann and Diehl's (2006) parameterizations, the contact activation is parameterized as follows:

$$\frac{dN_{CNT}}{dt}(m^{-3}s^{-1}) = m_{io} D_{ap} 4\pi r_m N_{a,cnt} \frac{N_l^2}{\rho_a q_c} \quad (1)$$

where $\frac{dN_{CNT}}{dt}$ is the rate of ice-crystal number production via contact freezing, m_{io} is the original mass of a newly formed ice crystal, ρ_a air density, q_c the mass mixing ratio of droplets, N_l the number mixing ratio of droplets, D_{ap} ($m^2 s^{-1}$) is the Brownian aerosol diffusivity, r_m is volume mean droplet radius and $N_{a,cnt}$ (m^{-3}) is the number concentration of contact nuclei. In Lohmann and Diehl's (2006) parameterizations, immersion and condensation-freezing activation is parameterized as follows:

$$\frac{dN_{IMM}}{dt}(m^{-3}s^{-1}) = N_{a,imm} \exp(T_0 - T) \frac{dT}{dt} \frac{\rho_a q_c}{\rho_w} \quad (2)$$

where $\frac{dN_{IMM}}{dt}$ is the rate of ice-crystal number production via immersion and condensation freezing, ρ_w water density, T air temperature, T_0 freezing air temperature. $N_{a,imm}$ (m^{-3}) the number concentration of immersion and condensation nuclei. For deposition nucleation, Möhler et al.'s [2006] parameterization calculates the deposition nucleation as follows:

$$\frac{dN_{DEP}}{dt}(m^{-3}s^{-1}) = N_{a,dep}(\exp[a(S_i - S_0)] - 1) \quad (3)$$

where $\frac{dN_{DEP}}{dt}$ is the rate of ice-crystal number production via depositional freezing, S_i saturation ratio with respect to ice, a and S_0 are non-dimensional empirical constants determined by chamber experiments, which are dependent on aerosol properties. Here, a and S_0 are set to 4.77 and 1.07, respectively, based on experiments for dust.

$N_{a,dep}$ is the number concentration of deposition nuclei (m^{-3}). This parameterization is applied to grid points with no cloud liquid to make sure only deposition nucleation is calculated.

Since we don't have observation data of ice nuclei and their properties including their chemical composition, we are not able to classify ice nuclei into contact nuclei, immersion and condensation nuclei, and deposition nuclei in a theoretical way. Hence, instead of obtaining $N_{a,cnt}$, $N_{a,imm}$, and $N_{a,dep}$ from the number concentrations of ice nuclei (N_a) theoretically based on the chemical composition of ice nuclei or instead of dividing N_a into $N_{a,cnt}$, $N_{a,imm}$, and $N_{a,dep}$ theoretically based on the chemical composition of ice nuclei, in the simulations, to obtain individual $N_{a,cnt}$, $N_{a,imm}$, and $N_{a,dep}$ from N_a, we made a rough assumption that a third of N_a is to be each of $N_{a,cnt}$, $N_{a,imm}$, and $N_{a,dep}$ and this assumption satifies $N_a = N_{a,cnt} + N_{a,imm} + N_{a,dep}$.

The averaged ice-crystal number concentration over grid points with non-zero ice-crystal number concentration at each time step is at the order of magnitude of 0.1 - 1 cm^{-3} in the runs. This range of the concentration is consistent with Lohmann and Diehl (2006) whose parameterizations are used for ice-crystal heterogeneous nucleation in this study as described above. In Figure 6 in Lohmann and Diehl (2006), for predicted CDNC around the order of magnitude of 100 cm^{-3}, predicted ice-crystal number concentration varies between ~0.1 cm^{-3} and ~1 cm^{-3}; note that as seen in our response to the comment on line 402 below, CDNC in the runs is approximately between 100 and 1000 cm^{-3}. The consistency between this study and Lohmann and Diehl (2006) in terms of the range of ice-crystal number concentration indicates that ice-crystal number concentration in this study follows up well with the previous study whose ice-nucleation parameterizations are adopted by this study.

Line 241: What happens to aerosol from evaporating hydrometeors? If aerosol is recovered, information is lost, and I would not say that evolution is followed.

Aerosols in hydrometeors can come out of those hydrometeors and become present in the air when those hydrometeors containing those aerosols are entirely evaporated and disappear. In this study, this process is NOT considered. Instead, as described in text, at any grid points, immediately after clouds disappear entirely, aerosol size distributions and number concentrations recover to background properties that background aerosols at those points have before those points are included in clouds.

In this way, we can keep the concentrations of background aerosols outside clouds in the simulations at observed counterparts.

The corresponding text is revised as follows to remove confusion from the use of word "evolution":

(LL296-299 on p10-11)

In this way, we can keep concentrations of background aerosols outside clouds in the simulations at observed counterparts. This enables spatiotemporal distributions of background aerosols in the simulations to mimic those distributions that are observed and particularly associated with observed aerosol advection in reality.

Line 280: "However, background aerosol concentration acting as INP at each time step and grid point in the low-aerosol-s run is not different from that in the control-s run during the simulation period." This is a very surprising selection as throughout the manuscript the effect of aerosol on precipitation is discussed. Please change the wording and describe in more detail the temperature dependence of IN concentration.

In this study, we focus on effects of CCN, but not INP, on clouds and precipitation. This is because aerosols acting as CCN account for most of aerosol mass that affects clouds and precipitation, and those aerosols acting as CCN but not INPs are associated with major theories of aerosol-cloud interactions such as aerosol-induced invigoration of convection and intensification of gust fronts as described in "Introduction".

To clearly identify CCN effects on clouds and precipitation, we isolate CCN effects on clouds and precipitation by changing CCN concentrations only but not changing INP concentrations between the runs. To clarify this point, text is revised or added as follows:

(LL54-57 on p3)

This study examines the role played by aerosols which act as cloud condensation nuclei (CCN) in the development of clouds and precipitation in two metropolitan areas in East Asia that have experienced substantial increases in aerosol concentrations over the last decades.

(LL110-117 on p4-5)

This study aims to examine effects of the increasing aerosols, which particularly act as cloud condensation nuclei (CCN), and their advection on clouds and precipitation in East Asia. This study focuses on aerosols which act as CCN, but not ice-nucleating

particles (INPs), to examine those effects, based on the fact that CCN account for most of aerosol mass that affects clouds and precipitation, and CCN, but not INPs, are associated with above-described aerosol-induced invigoration of convection and intensification of gust fronts. Note that these aerosol-induced invigoration and intensification are two well-established major theories of aerosol-cloud interactions.

(LL335-337 on p12)

However, to isolate CCN effects on clouds, background aerosol concentration acting as INPs at each time step and grid point in the low-aerosol-s run is not different from that in the control-s run during the simulation period.

In addition to revised text above, other words and phrases are revised to clearly indicate that this study is about CCN effects on clouds and precipitation but not INP effects. See manuscript for this revision.

There is no temperature dependence of IN concentration. As described in text, IN concentration is determined by observed aerosol properties at the surface (e.g., PM, aerosol size distribution and chemical composition), the assumption about the vertical distribution of aerosol concentrations and the assumption about the ratio of the IN concentration to the CCN concentration as detailed in text.

In authors' reply to the reviewer's comment about "the temperature dependence for heterogeneous nucleation", we describe how heterogeneous nucleation is parameterized by considering factors including the temperature dependence of heterogeneous nucleation.

Line 320: What is the total number of stations? Agreement with observations seems to be very good. Would it be possible to add the locations of stations into maps to see how well those cover the simulated area?

The total number of stations in Seoul (Beijing) area is ~300 (600). The locations of stations are marked in Figure 2. Displaying all stations in Figure 2 makes it messy. So, the locations of selected stations are displayed in Figure 2. These stations are selected in a way to represent overall distribution patterns of all stations well. The marked locations in Figure 2 indicate that stations cover the simulation domain on land reasonably well.

343: What does "cumulative frequency distributions of precipitation rates" mean. How is rain rate cumulated. Also, more information is needed on the process used to extend the observations to fill the simulated domain.

1. About cumulative frequency distribution of precipitation rates

We classify precipitation rates at each time step and grid point in the whole domain and during the whole simulation period. The classified precipitation rates are put into corresponding bins of precipitation rates. Then, we count the number of those rates in each bin and the number in each bin is shown in Figure 6.

For example, let us assume that the minimum and maximum of precipitation rates over the whole domain and simulation period are 1 and 12, respectively, and we use a bin interval of 3. In this assumed situation, there are three bins. The first bin is between precipitation rates of 1 and that of 4, the second bin between 5 and 8 and the third bin between 9 and 12. Then, let us assume that there are 2 time steps during the whole simulation period and 2 grid points over the whole domain, and non-zero precipitation rates occur at all time steps and grid points. Then, there are 2 values of precipitation rates over the whole domain at each time step. Let us assume these values are as follows:

At the first time step:

The first grid point: 1

The second grid point: 7

At the second time step:

The first grid point: 6

The second grid point: 12

Then, there are “one count” of precipitation rate whose value is 1 for the first bin between 1 and 4, “two counts” of precipitation rates whose values are 6 and 7 for the second bin between 5 and 8, and “one count” of precipitation rate whose value is 12 for the third bin between 9 and 12. These “one count” or “two counts” in each bin correspond to “cumulative frequency of precipitation rates” in each bin. When the cumulative frequency in one of the bins is plotted together with that in the other bins as in Figure 6, this plot represents “cumulative frequency distribution of precipitation rates”.

2. About extrapolation/interpolation of observation data to grid points

Observation data are extrapolated or interpolated into each time step and grid point in the simulations. For these extrapolation and interpolation, the inverse distance

weighting (IDW) method is used. The method is one of popular ones for the extrapolation and interpolation and detailed at https://en.wikipedia.org/wiki/Inverse_distance_weighting. To indicate the IDW method used, the following is added:

(LL222-224 on p8)

In this study, the inverse distance weighting method is used for the extrapolation and interpolation of observation data including aerosol mass into grid points and time steps in the model.

402: The number of cloud droplets formed should be presented to see how high concentrations can be found from the clouds to estimate the formation efficiency of warm precipitation.

The following is added:

(LL473-475 on p16)

CDNC, which is averaged over grid points and time steps with non-zero CDNC, is 1050 and 352 cm^{-3} in the control-s and low-aerosol-s runs, respectively.

(LL634-636 on p21)

CDNC, which is averaged over grid points and time steps with non-zero CDNC, is 992 and 341 cm^{-3} in the control-b and low-aerosol-b runs, respectively.

403: Are the differences in condensation rate meaningful to produce changes in updrafts? The increase in the condensation rate is five order of magnitude smaller than the change in liquid water content, thus being much longer than the lifetime of a single convective cell. Or is the main reason for increased liquid water the decrease in the precipitation formation efficiency which together with an increase in the updraft mass flux increases the amount of liquid water at higher altitudes also. This effect is not analyzed at all. I would expect the droplet concentration even in the low aerosol case to be high enough to maintain the supersaturation with respect to liquid water very close to zero.

We found errors in the program calculating condensation, deposition and freezing rates and due to these errors, just the order of magnitudes of those rates is wrong. These errors are related to the conversion between gram and kilogram. With the corrected order of magnitudes as shown in Figures 8 and 12 in the new manuscript, the increase in condensation rates is around two orders of magnitude smaller than the

change in liquid water content. Hence, it is hard to say that the time scale of the increase in condensation rates is longer than the lifetime of a single convective cell.

We repeated the control-s and low-aerosol-s runs by fixing CDNC and droplet size only for condensation which is related to drops (or droplets) whose sizes are smaller than 40 micrometers in radius. As mentioned in one of our responses above, in the microphysical scheme adopted in this study, for the calculation of cloud liquid content and rain water content, drops whose radius is smaller (greater) than 40 micrometers in radius are treated to be droplets (raindrops).

The fixed CDNC and droplet size are the average CDNC and size over grid points and time steps with non-zero CDNC in the low-aerosol-s run. The fixed CDNC and droplet size are applied to both of the repeated runs and thus there are no differences in CDNC and droplet size only for condensation between the repeated runs. The repeated control-s and low-aerosols-s runs are referred to as “the control-fixed-s run” and “the low-aerosol-fixed-s run”. However, in these repeated runs, the predicted CDNC and sizes are applied to all of the other processes including collision and coalescence processes among drops or among raindrops or among raindrops and droplets. In these repeated runs, due to no aerosol-induced increases in CDNC and associated surface area of droplets for condensation, there are negligible aerosol-induced changes in condensation and updrafts as shown in supplementary Figure below for 12:00 LST when the MCS is at its mature stage.

There are aerosol-induced increases in cloud-liquid mass or content due to reduced autoconversion or decreases in the precipitation formation efficiency. These increases in cloud-liquid or droplet mass can induce more accretion of droplets by raindrops and thus precipitation by providing more droplets as a source of the accretion. However, there is an aerosol-induced decrease in precipitation between the repeated runs. The domain-averaged cumulative precipitation amount at the last time step is 11.2 mm and 12.3 mm in the control-fixed-s run and the low-aerosol-fixed-s run, respectively. This means that aerosol-induced decreases in precipitation formation efficiency and associated reduction in precipitation formation outweigh effects of autoconversion-reduction-induced increases in cloud-liquid mass on precipitation, leading to aerosol-induced reduction in precipitation, in the circumstances of negligible aerosol-induced changes in condensation and updrafts. This also means that there should be aerosol-induced increases in condensation, updrafts and associated increases in cloud liquid to induce aerosol-induced increases in precipitation by overcoming aerosol-induced reduction in the precipitation formation efficiency and associated reduction in precipitation formation, as seen in comparisons between the pair of the control-s and low-aerosol-s runs and that of the control-fixed-s and low-aerosol-fixed-s runs.

CDNC does not determine supersaturation solely. Environmental CAPE, which is controlled by a synoptic condition, and associated updrafts also affect supersaturation. For example, although CDNC is very high, there can be environmental CAPE and associated updraft speed that are high enough to maintain supersaturation with a significant magnitude. As mentioned in one of our responses above, the averaged CDNC over grid points and time steps with non-zero CDNC is 1050 and 352 cm^{-3} in the control-s and low-aerosol-s runs. Comparisons between the pair of the control-s and low-aerosol-s runs and that of the control-fixed-s and low-aerosol-fixed-s runs demonstrate that when the average CDNC changes from 352 cm^{-3} in the low-aerosol-s run to 1050 cm^{-3} in the control-s run, there are significant increases in condensation and associated updraft intensity. However, when the average CDNC is fixed at that in the low-aerosol run and does not vary from the low-aerosol-fixed-s run to the control-fixed-s run, there are negligible changes in condensation and updrafts. The time- and domain-averaged CAPE, basically determined by a given synoptic condition, is ~1000 J kg^{-1} in the control-s, low-aerosol-s, control-fixed-s, and low-aerosol-fixed-s runs. These four simulations indicate that a combination of CDNC, CAPE and associated updrafts in the low-aerosol-s run leads to a situation where supersaturation in the low-aerosol-s run is large enough to generate changes in condensation which are large enough to induce ~20 % changes in cumulative precipitation when CDNC increases from that in the low-aerosol-s run to that in the control-s run.

The control-s run is repeated again by increasing background concentrations of aerosols at each grid point and time step by a factor of 3.1; remember that the average background concentration of aerosols in the control-s run is higher than that in the low-aerosol-s run by a factor of 3.1. This repeated run is referred to as “the high-aerosol-s run”. In the high-aerosol-s run, CDNC and droplet size are not fixed and predicted CDNC and size are applied to both condensation and all of the other microphysical processes including collision and coalescence processes. Increases in condensation and updraft intensity are ~ 2.5 times smaller on average from the control-s run to the high-aerosol-s run than from the low-aerosol-s run to the control-s run. This leads to a situation where there is only ~5% increase in precipitation amount from the control-s run to the high-aerosol-s. Remember that there is ~20% increase in precipitation amount from the low-aerosol-s run to the control-s run. This indicates that as the reviewer pointed out, lower supersaturation due to higher CDNC in the control-s run than in the low-aerosol run leads to a situation where aerosol-induced increases in condensation and updraft intensity are smaller from the control-s run to the high-aerosol-s run than from the low-aerosol-s run to the control-s run. This means that reducing supersaturation due to increasing CDNC lowers the sensitivity of condensation, updraft and precipitation to increasing aerosol concentrations, which is in line with the reviewer’s argument. However, simulations here demonstrate that although supersaturation in the low-aerosol-s run can be considered low as the

reviewer pointed out, supersaturation in the low-aerosol-s run is at the magnitude with which increasing aerosol concentrations from the low-aerosol-s run to the control-s run can induce increases in condensation and updraft intensity significantly enough to in turn induce ~20% increases in precipitation.

Aerosol-induced increases in condensation and associated invigoration of updrafts in this study are consistent with the observational study of Koren et al. (2014) and the theoretical study of Igel and van den Heever (2021). Koren et al. (2014) and Igel and van den Heever (2021) showed that with more aerosol particles in clouds, there is more release of latent heat of condensation that induces invigoration of updrafts. In particular, Igel and van den Heever (2021) showed that in mixed-phase clouds, aerosol-induced increases in condensation play a more important role in the invigoration of updrafts than those in freezing.

References:

Koren, I., Dagan, G., & Altaratz, O. (2014). From aerosol-limited to invigoration of warm convective clouds. Science, 344(6188), 1143-1146.

Igel, A. L., & van den Heever, S. C. (2021). Invigoration or enervation of convective clouds by aerosols? Geophysical Research Letters, 48, e2021GL093804. https://doi.org/10.1029/2021GL093804

Seoul case
(control-fixed-s run minus low-aerosol-fixed-s run)

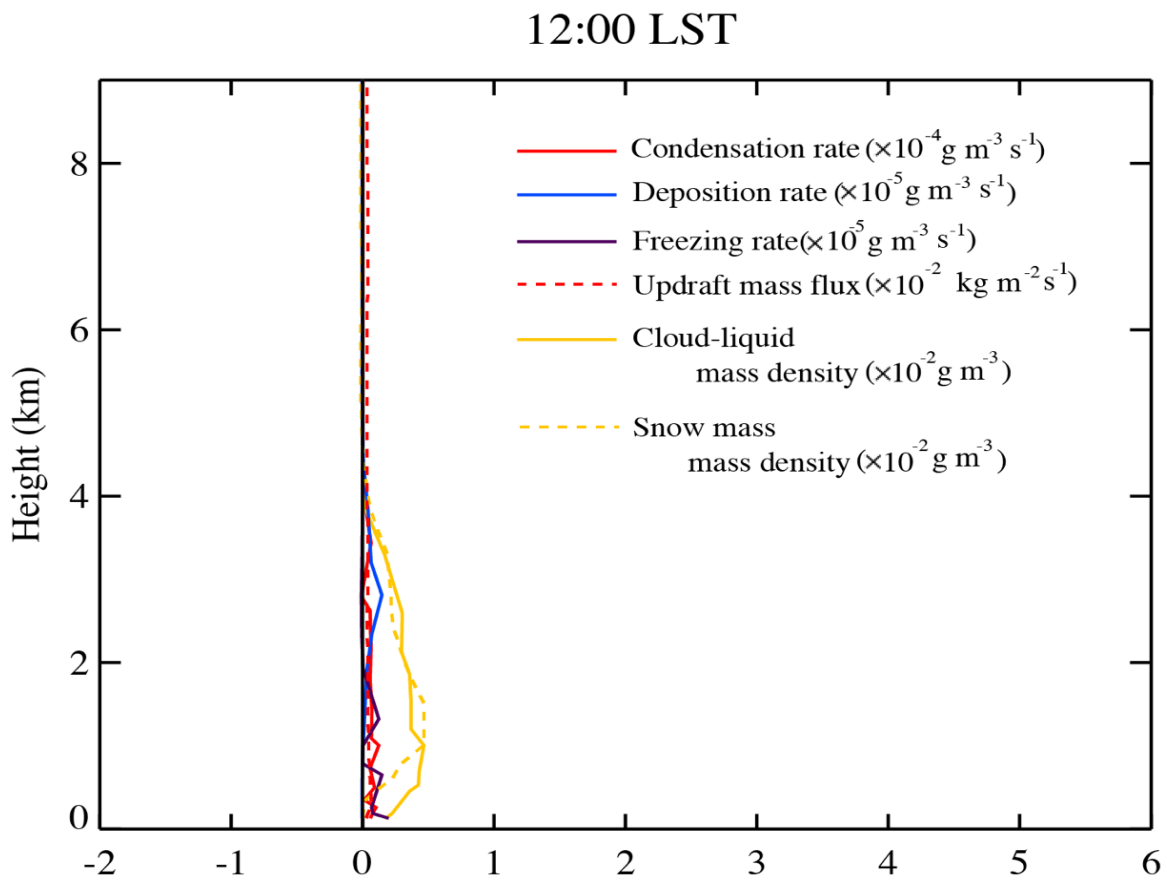

Supplementary Figure. Vertical distributions of differences in the area-averaged condensation, deposition and freezing rates, and cloud-liquid and snow mass density, and updraft mass fluxes between the control-fixed-s and low-aerosol-fixed-s runs at 12:00 LST.

Line 422: It is surprising that differences in freezing rates are so small. Does it include also the ice/snow formed in collisions between liquid and frozen hydrometeors? Delayed warm precipitation formation should increase the liquid water content in mixed phase part of the cloud and thus provide more liquid for freezing also. Overall, can you estimate how big fraction of precipitation is formed through cold and warm processes and how it is changing with changing CCN concentration?

We found that we missed some of riming processes in the calculation of freezing rates. We re-calculated freezing rates by including all riming processes or collision processes between liquid and frozen (or solid) hydrometeors. These re-calculated freezing rates are reflected in Figures 8 and 12 and corresponding text in the new manuscript.

As described in text, CCN-induced increases in condensation in turn induce CCN-induced increases in updraft intensity. These increases in updraft intensity eventually induces CCN-induced increases in deposition for the Seoul case. For the Seoul case, over the whole simulation period and domain, differences in the average freezing rate between the control-s and low-aerosol-s runs are one to two orders of magnitude smaller than those in condensation and deposition rates as seen in Figure 8 in the new manuscript with the corrected freezing rates, although freezing rate increases with increasing CCN number concentrations. Hence, it is differences in condensation and deposition but not those in freezing that control differences in the mass of hydrometeors between the runs for the Seoul case.

It Is found that 61 (35) % of precipitable hydrometeors is generated by warm processes, while 39 (65) % of precipitable hydrometeors is generated by cold processes in the control-s (low-aerosol-s) run. We see that the ratio of generation of precipitable hydrometeors by warm processes to that by cold processes increases with increasing aerosol or CCN concentrations between the runs. Here, it should be emphasized that cold processes for each of the runs are predominantly controlled by deposition but not by freezing. The time- and domain-averaged freezing rate is ~one to ~two orders of magnitude smaller than deposition rate in each of the runs. This leads to above-mentioned negligible roles of freezing in differences in the mass of hydrometeors between the runs as compared to those roles of deposition for the Seoul case.

Line 658: Binned microphysics is employed, so there should not be a need for autoconversion as cloud droplet grow through coagulation coalescence to precipitation?

The corresponding text is revised as follows:

(LL766-771 on p26)

This and lower efficiency of collision and collection among droplets enable the control-b run to have a larger amount of cloud liquid or droplets as a source of evaporation. This in turn enables more droplet evaporation, more associated cooling and stronger downdrafts, although less rain evaporation is in the control-b run particularly for the period from 17:00 LST to 19:00 LST (Figure 17).

Lines 673-763: This is very interesting analysis and the change in the energy flow seems quite strong. The static energy itself is probably only slightly affected by aerosol (or is there more water in the PBL), so the change comes from the wind vector or how the averaging is done. As the selection of limiting value for areas A and B is quite arbitrary but still affecting the size of A and B areas, I would expect that the differences between different aerosol cases change when different criteria for areas A and B is employed. And thus, averaging affect the outcome. Maybe using net flux instead of domain averaged values could make this more convincing.

Here, we just want to emphasize that limiting values for aeras A and B are not arbitrary and based on Figure 15. We want to understand how the tipping precipitation rates of ~2 and ~12 mm hr^{-1} between the control-b and low-aerosol-b runs are formed; see text for the details of the tipping precipitation rates. Based on Figure 15 and associated analysis, we find correspondence between the tipping precipitation rates and condensation rates. This correspondence indicates that condensation rates below ~3 × 10^{-3} g m^{-3} s^{-1} and above ~10 × 10^{-3} g m^{-3} s^{-1} are correlated with precipitation rates below ~2 mm hr^{-1} and above ~12 mm hr^{-1}, respectively, while condensation rates between ~3 and ~10 × 10^{-3} g m^{-3} s^{-1} are correlated with precipitation rates between ~2 and ~12 mm hr^{-1}; see text for the details of this correspondence. As a way of understating the formation of the tipping precipitation rates, we are interested in the redistribution of precipitation between areas with precipitation whose rates are higher than ~12 mm hr^{-1} and those with precipitation whose rates are between ~2 and ~12 mm hr^{-1}. To examine this redistribution, based on the correspondence, we examine areas (or area A) with condensation rates from 3×10^{-3} g m^{-3} s^{-1} to 10 ×10^{-3} g m^{-3} s^{-1} which correspond to precipitation whose rates are between ~2 and ~12 mm hr^{-1} and areas (or area B) with condensation rates above 10×10^{-3} g m^{-3} s^{-1} which correspond to precipitation whose rates are above ~12 mm hr^{-1}.

As shown in Figure 15, there is a standard deviation of the precipitation rate for each column-averaged condensation rate; note that to determine the above-described correspondence between the tipping precipitation rates and condensation rates, the mean precipitation rate for each condensation rate in Figure 15 is used. To check the robustness of results in Section e “moist static energy”, this standard deviation and an associated range of precipitation rate (but not one mean precipitation rate) for each condensation rate are considered; here, the range extends over the standard deviation for each condensation rate and starts from the bottom of a vertical bar to the top of the bar in each condensation rate in Figure 15. Based on the range of precipitation rate, condensation rate corresponding to precipitation rates of ~12 mm hr^{-1} (~2 mm hr^{-1}) can vary from ~9 ×10^{-3} g m^{-3} s^{-1} to ~12×10^{-3} g m^{-3} s^{-1} (from ~1 ×10^{-3} g m^{-3} s^{-1} to ~4×10^{-3} g m^{-3} s^{-1}); here, the range of precipitation for each of condensation rates between ~9 ×10^{-3} g m^{-3} s^{-1} and ~12×10^{-3} g m^{-3} s^{-1} includes the precipitation rate of ~12 mm hr^{-1},

while the range of precipitation for each of condensation rates between ~1 $\times 10^{-3}$ g m^{-3} s^{-1} and ~4$\times 10^{-3}$ g m^{-3} s^{-1} includes the precipitation rate of ~2 mm hr^{-1}. We repeated the analysis in Section e by applying these variations of condensation rate to the determination of areas A and B. Here, based on the variations of condensation rate, we used condensation rate of each of 9, 10, 11, and 12 $\times 10^{-3}$ g m^{-3} s^{-1} as the minimum (maximum) condensation rate for area B (area A) and condensation rate of each of 1, 2, 3 and 4 $\times 10^{-3}$ g m^{-3} s^{-1} as minimum condensation rate for area A. Hence, there are 16 sets of the repeated analysis, considering the combination of 4 values of minimum (maximum) condensation rate for area B (area A) and 4 values of minimum condensation rate for area A. These sets demonstrate that results in Section e, which involve the net positive flux of the energy from area A to area B, are robust to the variation of condensation rates used to determine areas A and B.

In text, we describe that CCN-induced more condensation intensifies updrafts in area B, associated wind convergence and flow of moist static energy by wind convergence from area A to area B more in the control-b run than in the low-aerosol-b run. Hence, as the reviewer stated, changes in wind convergence or wind affects the flow of moist static energy. We want to reiterate that these changes in wind are triggered by changes in CCN concentrations and associated condensation. When we repeated the control-b and low-aerosol-b runs by removing latent heating by condensation in area B from 16:30 LST on, we find the absence of more net positive flux of the moist static energy from area A to area B in the repeated control-b run than in the repeated low-aerosol-b run, and no formation of the tipping precipitation rates in these repeated runs. These repeated runs demonstrate that CCN-induced differences in latent heating by condensation in area B trigger differences in wind convergence and associated flux or flow of the moist static energy from area A to area B between the control-b and low-aerosol-b runs, and form the tipping precipitation rates, as described in Section e.

Following the comment here and the other reviewer's comment, the total or net fluxes replace the domain-averaged fluxes in text. The corresponding text is revised accordingly.

Figure 8: Is it only snow here, or does it include all frozen hydrometeors? Also, the change in cloud fraction should be presented as all variables are presented area averaged. In addition, information related to temperature profile, at least the melting and heterogeneous freezing levels would help in understanding the changes at different altitudes.

In Figures 8 and 12, we added differences in the mass of other precipitable hydrometeors (i.e., raindrops and hail particles) between the runs. Accordingly, text is revised. Here, for the simplicity of the display, hail particles include graupel particles.

Also, want to note that snow mass in Figures 8 and 12 includes the ice-crystal mass for the simplicity of the display.

The melting and freezing levels are nearly at the level where temperature is 0 ºC. The level with the temperature of 0 ºC is marked in Figures 8 and 12 and accordingly, the following text is added:

(LL468-469 on p16)

In Figure 8, horizontal black lines represent the altitudes of freezing and melting.

(LL629-630 on p21)

In Figure 12, horizontal black lines represent the altitudes of freezing and melting.

Regarding the cloud fraction, the following is added:

(LL463-465 on p16)

Cloud fractions are 0.32 (0.30), 0.85 (0.82), 0.93 (0.92) and 1.00 (1.00) in the control-s (low-aerosol-s) run at 03:20, 03:40, 06:00 and 12:00 LST, respectively. We see that cloud fraction does not vary significantly between the runs.

(LL626-629 on p21)

Cloud fractions are 0.12 (0.11), 0.25 (0.22), 0.36 (0.32), 0.43 (0.40) and 0.48 (0.47) in the control-b (low-aerosol-b) run at 14:20, 15:40, 16:00, 17:20 and 19:00 LST, respectively. Here, we see that cloud fraction does not vary significantly between the runs.

To respond to a general comment above about changes in cloud-top heights with changing aerosols, the following is added. In the following, cloud depth, which is equivalent to cloud-top height, is presented.

(LL483-485 on p16-17)

This eventually leads to a situation where the maximum cloud depth is ~ 7 km in the control-s run and this depth is ~5 % deeper than that in the low-aerosol-s run for the whole simulation period.

(LL640-642 on p22)

These updrafts enable the maximum cloud depth to be ~ 12 km in the control-b run and this depth is just ~1 % deeper than that in the low-aerosol-b run for the whole simulation period.

Figure 9: This is complicated figure, and it is difficult to see what happens. Maybe the quality good be improved through decreasing the number of panels.

Figures 9c, 9d, 9g, 9h, 9i, 9j, 9m, 9n, 9q, 9r, 9w,9x,9y, and 9z are removed and text is revised accordingly.